International Journal of Engineering Trends and Technology
ISSN: 2231 – 5381 / https://doi.org/10.14445/22315381/IJETT-V71I3P216

Volume 71 Issue 3, 155-167, March 2023

Original Article

Rapturous Chimp Optimization-based Feed-Forward Neural Networks for Autism Spectrum Disorder Classification

B. Suresh kumar[1], D. Jayaraj[2]

[1]*Department of Computer and Information Science, Annamalai University, Tamilnadu, India*
[2]*Department of Computer Science and Engineering, Annamalai University, Tamilnadu, India*

[1]*Corresponding Author : sureshaucis@gmail.com*

Received: 25 October 2022 Revised: 06 March 2023 Accepted: 12 March 2023 Published: 25 March 2023

Abstract *- Observational and interview-based evaluations are used to diagnose autism spectrum disorder (ASD), but these methods are labor-intensive, highly subjective, and fraught with doubts about their validity and reliability. Artificial intelligence's deep learning subfield focuses on creating useful new programmes in many fields. Its great classification accuracy makes it a popular tool for mining large datasets for previously unseen patterns and insights. This paper proposes a bio-inspired optimization-based deep learning technique to perform robust classification of ASD with neuroimaging data, namely Rapturous Chimp Optimization-based Feed-Forward Neural Networks (RCO-FFNN). Fitness evaluation, exploration, and exploitation play a vibrant role in RCO-FFNN to achieve better accuracy. In RCO-FFNN, social incentives are preferred to detect ASD and non-ASD. The Autism Brain Imaging Data Exchange II (ABIDE-II) dataset, a worldwide multisite collection of functional and structural brain imaging data, is used to test the RCO-FFNN's efficacy. Results make an indication that the RCO-FFNN outperforms current classifiers in terms of Classification Accuracy, F- Measure, Fowlkes-Mallows Index, and Matthews Correlation Coefficient.*

Keywords *- Autism, Chimp, Classification, Feed-Forward Neural Network, Optimization.*

1. Introduction

The field of Medical Informatics examines how computer science and healthcare might work together to improve human health. Two different types of medical data are brought together by medical informatics to facilitate field research. Both the medical history and the images collected for it have unique characteristics. Pixels in digital images represent actual parts of objects captured by various imaging technologies. In contrast, a patient's biomedical record is built from medical test records. Because of their unique characteristics, biomedical records and imaging data require different research approaches. Researchers and their tools have mined biomedical records. Imaging modalities generate medical picture data. The challenge in this area is determining which areas of the human body are afflicted by a certain disease and then classifying the extracted images into comparable patterns. Processes involved in medical image classification are provided in Figure 1.

Extracting features from a medical picture, representing them, and deciding which ones to utilize for classification are the first two steps in the medical image analysis process; the third is classifying the features and the image. Moreover, picture classification plays a crucial part in computer-aided diagnostics. It is important to note that three key phases are involved in medical picture classification: pre-processing, feature extraction, and classification. Once the picture has been processed, the features of interest must be extracted to analyse the data. To do this, the pattern classification system converts the input variables into the corresponding output variables.

The selection of methodologies and strategies for utilizing the results of (i) image processing, (ii) recognition of patterns, (iii) classification strategies, and (iv) outcome of classification into medical expert knowledge poses a significant difficulty for image analysis jobs. The primary goal of medical picture classification is to determine not only a high level of accuracy but also to pinpoint the exact anatomical locations of illness. Better clinical care can be achieved in the future by developing an automated diagnosis method using picture data. Given that translating the results of picture classification studies into the specialized knowledge of medical professionals remains a significant problem, there is still much room for exploration in image classification research.

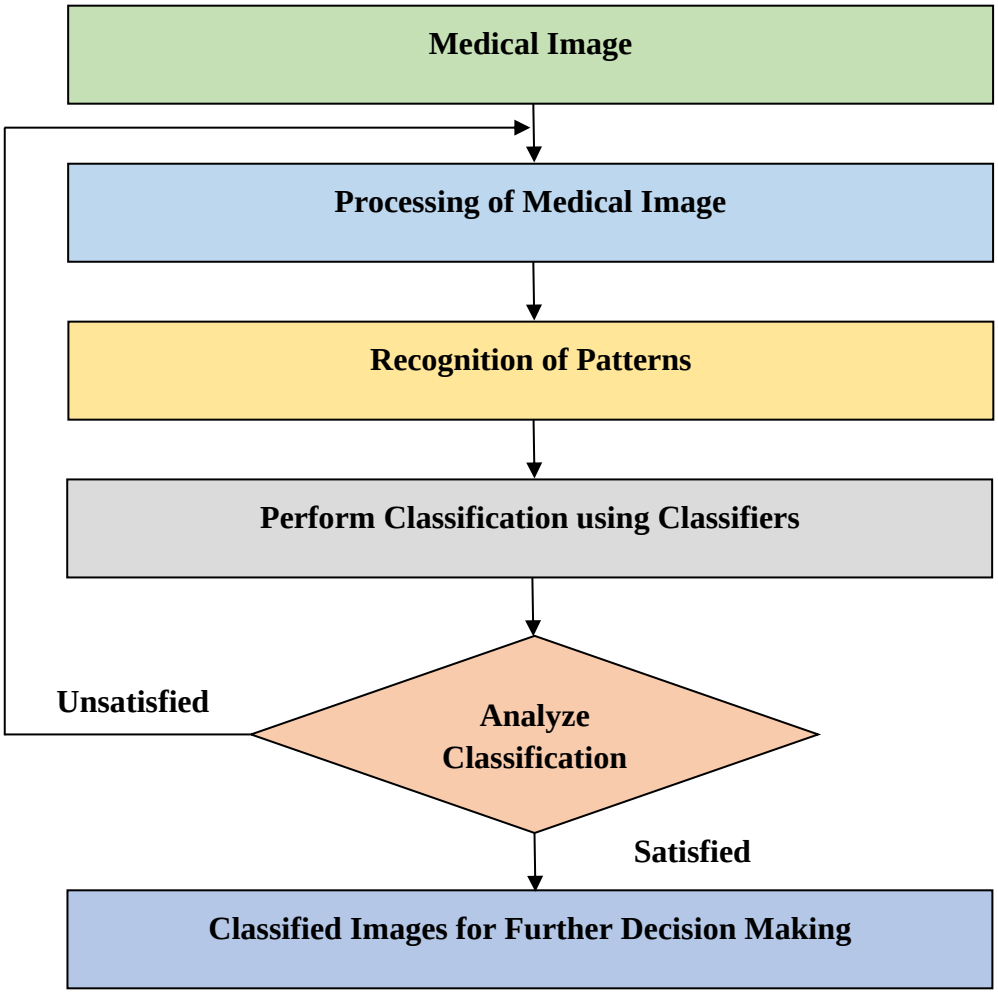

Fig. 1 Image Classification Process

1.1. Autism

Involvement in highly structured routines and limited, repetitive behaviour patterns, interests, or activities are hallmarks of Autism Spectrum Disease (ASD), a neurodevelopmental disorder [1]. Reciprocal social contact may be impaired because children with ASD have trouble with functional initiatives, social initiatives, and socially appropriate replies. Most intervention studies employ a wide range of therapy methods to help children with ASD improve their social communication skills, which is considered a key weakness in this population [2]. With a total population of close to 1.3 billion, India is home to over a third of the world's youth population. According to estimates, millions of individuals in India may have autism spectrum disorder. The cited research on ASD largely relies on data from hospitals. Thus, we do not know how common the illness is in India [3]. Its prevalence in communal settings has been the subject of very few investigations. It is also challenging to assess the true prevalence of ASD due to the inconsistent use of properly validated and translated autistic diagnostic methods.

Moreover, ASD is underrecognized since early diagnoses are often delayed. Children with ASD require more health care, educational assistance, and rehabilitative services, all of which have direct and indirect financial repercussions for the country. The incidence of ASD in India has not been the subject of comprehensive reviews [4], [5].

Social and communication skills are affected by autism spectrum disorder. This disorder, which can have either a hereditary or environmental root, affects the neurological system and, in turn, the mind, heart, and body [6]. The extent and intensity of its symptoms are quite variable. Difficulties in communicating, especially in social situations, compulsive interests, and repeated mannerisms, are signs of someone who has autism. ASD must be identified with a thorough evaluation. As part of this process, we use child psychologists and other trained specialists to conduct a comprehensive examination and a battery of tests to determine the best course of action [7], [8]. The Autism Diagnostic Interview-Revised (ADI-R) and Autism Diagnostic Observation Schedule Revised (ADOS-R) are

two examples of standard diagnostic tools. However, these are time-consuming and labour-intensive due to their length and complexity. ASD affects a sizable percentage of children. Although early detection is possible in most situations, the main stumbling block is the subjectivity and tedium of current diagnosing processes [9]. This means that from the moment a diagnosis is suspected to the time it is confirmed, patients may expect to wait at least 13 months. Due to the high diagnostic time and ever-increasing demand for appointments, paediatric clinics across the country are operating at or near capacity. Early diagnosis and treatment of ASD are vital since they can reduce or relieve symptoms to some extent, increasing the level of well-being of the individual affected [10]. However, due to delays in raising concerns and receiving an official diagnosis, much time is wasted while the illness goes unidentified. In addition to improving the timeliness and precision of risk assessments for autism spectrum disorder (ASD), machine learning techniques would be useful in streamlining the whole diagnostic process and speeding up the delivery of much-needed therapy to families [11], [12].

1.2. Problem Statement

ASD is a disorder that affects how a person grows and develops. Its symptoms appear early in life, but people of any age can have it. ASD is a mental condition characterized by social interaction, communication, and language impairments. However, its effects can be mitigated or eliminated if detected early. The intensity and variability of ASD symptoms and the co-occurrence of these symptoms with those of other mental illnesses make it difficult to make an accurate diagnosis at an early stage. As deep learning techniques are being used in more areas, doctors can now get help identifying ASD at an earlier age. The necessity for an automated method to predict ASD originates from the difficulty of human clinicians in isolating and focusing on the most important factors in making such a diagnosis. The cost of diagnosing ASD keeps increasing daily and can be cut with deep learning and optimization strategies.

1.3. Objective

The primary goal of this research is to propose a classification algorithm, namely Rapturous Chimp Optimization-Based Feed-Forward Neural Networks, that can reliably detect the presence of ASD in ABIDE II dataset, which holds fMRI scan images.

1.4. Organization of the Paper

The processes involved in digital image processing, ASD, the problem statement, and the objective of the research are discussed in Section 1. Section 2 examines the existing research on how to classify ASD. Section 3 presents the novel bio-inspired deep learning method for ASD diagnosis. A brief overview of the ABIDE II data collection is provided in Section 4. Section 5 provides the evaluation metrics used to assess how well the suggested classifier performs compared to other classifiers. Discussions of the result are presented in Section 6. In Section 7, the conclusion with future enhancements is discussed.

2. Literature Review

"Automatic Imitation" [13] examines the animacy and perception belief based on the brain paradigm. The top-down and bottom-up beliefs are manipulated to suppress the animacy. Results are generated using neural and behavioral responses, and behavioral analysis is carried out. The imitative flexibility is examined biologically, results are generated, and ASD is predicted. "Adaptive Independent Subspace Analysis ($AISA$)" [14] is employed in the current study to discover the electroencephalogram tasks from the MRI scan. Results are tested with an image texture analysis method, and different matrices are obtained. The features are fetched and mapped in the feature space in $2D$.

The results are generated and tested with the cross-validation method. "Robot Teleoperation" [40] is used in the current study of ASD detection for children with the incorporation of robot behavior. The behavioral feature set of robots is integrated into the architecture and explored with human intervention. The motion structures are retrieved and evaluated with the autistic child's behavioral structures, and the interaction is demonstrated with training and testing samples. "Multifractal Analysis" [16] is applied in the monitoring task of attention deficit hyperactivity disorder ($ADHD$) in the proposed study. Features essential for analysis are extracted, and arithmetic recognition of task are generated using Higuchi fractal dimension spectrum ($GHFDS$) method. Recognition accuracy is obtained from single and multi-channel algorithms, and ranking is provided using channel ranking measures.

"Emotion-based Frames Extraction" [17] is innovated in the proposed study to demonstrate the training for children with ASD. The classifier for hypothesizing the training is performed, and the probability scores from the different classifiers are fetched. The game sessions are detected properly, and classifier performance is portrayed compared with other existing techniques. The "Multiresolution Variable Selection" [18] method with Bayesian probit regression architecture is proposed for the detection of ASD.

Markov Chain Monte Carlo ($MCMC$) algorithm is applied for variable selection, and two levels of priors for structural data are incorporated. The anatomical brain regions have functional connectivity, voxels are selected, and $RS-FMRI$-based data are used for evaluation. Simulation results are executed and compared with existing techniques. "Source localization from EEG using independent component analysis" [19] is applied for understanding ASD in neurobiological order for the proposed study.

The active regions are detected that are closer to fMRI. The time differing connectivity is estimated by translating the EEG resolution, and analysis is performed. The EEG is used to track the impact of ASD diagnosis and its treatment stage for further investigation. "Multiplayer Interaction Platform" [20] is developed along with the virtual reality of eye-tracking method for predicting ASD individuals. Participants of both ASD and TD are involved in the study, and results are generated in every participant group. The eye-gaze-based data are used based upon the looking pattern and performance portrayed as $GROUPASD$ and $GROUPTD$.

"Multi-Robot System" [21] is proposed in the current study for handling robot communication with autistic patients in single and multi-level. The robot is imitated the visual space, and findings are detected. Results are generated by using the brain and eye contact of both male and female participants. Accuracy of right space and left visual space is obtained, and performance is detected. Power Spectral Density is acquired to measure the hemisphere of the right-side brain of ASD individuals. "Multi-Robot Therapy" [22] with three Interaction frameworks called, Stage-1 ($Human - Human$), Stage-2 ($Human - Robot$), and Stage-3 ($Robot - Human$) is designed in the proposed study for enhancing the communication level of autistic children. Two command sets called: Controls and Evaluations are integrated at three levels. Multi-human communication is enabled, and joint attention is improved. Using the Childhood Autism Rating Scale value, the technique is validated. "Revised Psychoeducational Evaluation Scale" [23] is applied for evaluating the web system to enhance learning strategy in predicting ASD.

Different cognitive developmental areas are considered and the method called, Treatment and Education of Autistic Communication are applied to creating digital learning technology. The technique's performance is evaluated, and results are classified as Failures, Emergent, and Success. "Image Generator" [24] is designed to generate brain images in a single volume with the voxel time point. Deep Learning approaches are used for classification and ensemble together. The cross-validation technique is applied to validate the solutions, and a comparison is carried out. Pre-processing is also done to remove redundant pipelines and outperform them better than baseline techniques.

"Eye Tracking" [25] datasets are introduced in the current study to diagnose ASD individuals. They cover both the high-level to low-level functioning of autism. Also, the validation projects that used the gaze dataset can provide a way to handle a small number of datasets, and simulation needs to be carried out for enhancement. "Multi-Class ASD Classification" [26] is used to determine the ASD patients, and the features are extracted initially using the patch-based functional correlation tensor technique. Using multi-source domain adaptation, the source domains are turned into target space, and a multi-view classifier called multi-view sparse representation is developed to enable the diagnosis level. Experimental results are generated to show the effectiveness of the technique. **"**Eye-Movement Behaviors" [27] predict the ASD problem among children. Different participants with ASD and TD individuals are explored by differentiating into two groups, and the interaction between child-robot is increased. K-means clustering groups the gaze locations and determines the attention level. Results are generated based on the eye behavior with and without ASD. Successful applications of bio-inspired optimization have expanded into new fields like advanced networking [28]–[37], cyber security, medical image mining, share market prediction, etc.

An approach called "Genetic-Evolutionary Random Support Vector Machine ($GERSVM$)"[38] is developed, in which a group of SVMs chooses samples and features at random. Alterations are made to the genetic evolution, and the reliability of the categorization system is checked. To aid in diagnosing ASD, resting-state $fMRI$ is utilized to locate aberrant brain areas. Recursive Cluster Elimination-based Support Vector Machine ($RCE - SVM$) falls under the category of machine learning classification approach that is used by "Functional Connectivity Complex Network Measures ($FC - CNM$)" [15, 39] to assess the prediction efficiency of conventional connectivity and complex network measures acquired from the ABIDE dataset. $RCE - SVM$ was used to examine the prediction performance of three distinct feature sets: (1) Functional Connectivity, (2) Complex Network Measures, and (3) a combination of both 1 and 2. $FC - CNM$ has three stages: Clustering features, calculating the feature's relevance for cluster classification, and removing clusters with minimal scores using RCE.

3. Rapturous Chimp Optimization-based Feed-Forward Neural Networks

3.1. Feed-Forward Neural Networks

Artificial Neural Networks are mathematical models that, like the human brain, consisting of layered structures representing linked networks of neurons. Synapses connect each neuron in one layer to every other neuron in another layer below and above it (i.e., in a one-to-many manner). The learning process alters the original weights assigned to these links, which were randomly generated.

The input layer refers to the initial layer of a network architecture, which is in charge of taking in data. Similarly, the final layer is referred to as the output layer since it provides the final results. There may be nil, one, or several concealed levels depending on the circumstances. Neural network architects seek to accelerate learning by determining the optimum layer thicknesses. The number of input neurons is proportional to the number of characteristics of the item

under the analysis. In contrast, the output neurons count is proportional to the class count, and the objects are sorted based on the same.

Each neuron takes an input value, applies an activation function, and transmits the resulting signal to the layer below it. The s^{th} neuron in the a^{th} layer receives the input signal by following the Eqn. (1):

$$e_s^a = \sum_{w=1}^{t} n_{sw}^a q_w^{a-1}, \tag{1}$$

The weight of the link between the s^{th} neuron of the a^{th}layer and the $w^{th}$the neuron of the preceding layer is n_{sw}^a, and the value of the output signal from the w^{th} the neuron of the previous layer is q_w^{a-1}. The signal produced by the s^{th} the neuron is expressed as Eqn. (2):

$$q_s^a = g(e_s^a) = g\left(\sum_{w=1}^{t} n_{sw}^a q_w^{a-1}\right). \tag{2}$$

The number of activation functions (i.e., threshold function used for transferring) is rather large. A bipolar linear function is a popular option to achieve activation, and it is mathematically expressed as Eqn. (3):

$$g(e_s^a) = \frac{2}{1+h^{-\delta e_s^a}} - 1 = \frac{1-h^{-\delta e_s^a}}{1+h^{-\delta e_s^a}} \tag{3}$$

where δ is a factor that modifies the activation function's "width" (i.e., the convergence rate).

It is necessary to train an artificial neural network in ASD identification after it has been constructed. ANNs can learn by making precise changes to the weights of connections between neurons. $FFNN$ employs a back-propagation strategy which is a training approach in which the values of the connections are modified sequentially from the output layer to the input layer. The information placed into any $FFNN$ always travels opposite (i.e., reverse direction). The training aims to reduce the loss function for each element in the training set (F). Every time a neural network is fed, the obtained outputs are compared with the predicted outputs, which are part of the training set and are introduced into the first layer via input synapses. The loss function represents the distinction between the expected and observed values. Average Standard Deviation was calculated using Cost or Pass Loss can be used to determine the similarity present in Log Degradation. When expressed in terms of MSE, the total training set error may be stated as Eqn. (4):

$$H = \sum_{F}\sum_{s=1}^{t}(y_s - q_s)^2 \tag{4}$$

where t is a vector dimension indicating the count of neurons present in the output layer, y_s is the predicted value at the s^{th} scalar position, and q_s is the actual value at the s^{th} scalar position. Adjusting synaptic weights begins at the output layer and works on the way back via the hidden levels until it reaches the input layer. The calculation for adjusting the weight is expressed as Eqn. (5):

$$n_{sw}^a = n_{sw}^a + \alpha \nabla n_{sw}^a, \tag{5}$$

where α indicates a rate of learning, and its coefficient is fully utilized to correct errors, and ∇n_{sw}^a denotes the gradient of the synapse's weight error, and Eqn. (6) depicts the same.

$$\nabla n_{sw}^a = \frac{\partial H}{\partial n_{sw}^a} = \frac{1}{2}.\frac{\partial H}{\partial e_s^a}.2.\frac{\partial e_s^a}{\partial n_{sw}^a} = 2\theta_s^a q_w^{a-1}, \tag{6}$$

For the layer number a, the input signal to the s^{th} the neuron is denoted as θ_s^a, while the output signal from the w^{th} neuron in the preceding layer is denoted as q_w^{a-1}. Finally, A^{th} layer will equalize at θ times, and Eqn. (7) represents the same.

$$\begin{aligned}\theta_s^A &= \frac{1}{2}.\frac{\partial H}{\partial e_s^a} = \frac{1}{2}.\frac{\partial (y_s^A - q_s^A)^2}{\partial e_s^a} \\ &= g'(e_s^a).(y_s^A - q_s^A),\end{aligned} \tag{7}$$

wherein $g'(e_s^a)$ represents the differential of the input signal to the corresponding s^{th} output neuron, performed using the activation function. Here, the value is mostly based on the deviation (i.e., error) between the expected and observed outcome values. Numerals used in the θe of the other levels are derived from those of earlier phases, and Eqn. (8) depicts the same.

$$\begin{aligned}\theta_s^A &= \frac{1}{2}.\frac{\partial H}{\partial e_s^a} = \frac{1}{2}.\sum_{w=1}^{T_{a+1}}\frac{\partial H}{\partial e_w^{a+1}}\frac{\partial e_w^{a+1}}{\partial e_s^a} \\ &= g'(e_s^a)\sum_{w=1}^{T_{a+1}}\theta_w^{a+1} n_{sw}^{a+1},\end{aligned} \tag{8}$$

where T_{a+1} is the total number of neurons in the$(a+1)^{th}$ layer.

3.2. Rapturous Chimp Optimization (RCO)

The chimpanzees have both fission and fusion in their society. Different parts of society are combined in different proportions at different times. Talents and obligations are not static for members of chimpanzee society; rather, they are constantly developing. This is taken into account by the optimization algorithm, which suggests different varieties of groups. Each of these groups uses its own set of skills to explore the search space for a solution. The four different sorts of chimpanzees are (i) drivers $(Drvr)$, (ii) barriers $(Barr)$, (iii) chasers $(Chsr)$, and (iv) attackers $(Atkr)$. Together, they are crucial to a successful investigation. The $Drvr$'s keep an eye out for their quarry but make no moves

to catch any of them. There is no way for prey to escape since the obstacles have effectively built a dam in the forest. $Atkr$ need to be swift on their feet if they want to have any chance of catching their prey. Last but not least, $Atkr$ plot their attacks according to where they anticipate their prey to emerge from the lower canopy. To be effective, $Atkr$'s must be able to predict with pinpoint accuracy what their target will do next.

Consequently, after a successful hunt, $Atkr$'s are given more food (i.e., meat). Attacking is a crucial duty that increases with maturity, intelligence, and strength. Chimpanzees can also switch roles inside the hunt or remain the same throughout. Chimpanzees are known to engage in social support, sex, and grooming exchanges, including bartering meat. A critical mind may indirectly impact hunting by opening up previously unexplored avenues for success. It is assumed that only humans and chimpanzees use social incentives. Chimpanzees greatly benefit from this trait compared to other species of social predators. In addition, the chimpanzees' sexual urge causes them to act irrationally in the pivotal stage of the hunt when they abandon all other pursuits in favor of the food. Chimpanzees' unique behavior of social hunting may be divided into two phases: (i) "exploration," which requires pursuing, impeding, and chasing the prey, and (ii) "exploitation," which entails attacking the victim (i.e., prey).

3.2.1. Chimpanzee Driving and Chasing toward Prey

Prey is sought during the analyzing stages with the available resources. The prey's movement direction and speed can be statistically simulated using Eqn. (9) and Eqn. (10).

$$y = \sum \left| U.P_{prey}(f) - c.p_{chimp}(f) \right| \tag{9}$$

$$P_{chimp}(f+1) = P_{prey}(f) - d.y \tag{10}$$

where f indicates the count of the current iteration, $d, c,$ and u denote the coefficient vectors, and p_{prey} and p_{chimp} denote the prey and chimp's respective position (i.e., x and y coordinates) vectors. Eqn. (11), Eqn. (12), and Eqn. (13) represent the computation of vectors $d, c,$ and $u,$ respectively.

$$d = 2.g.b_1 - d \tag{11}$$

$$u = 2.b_2 \tag{12}$$

$$c = \text{chaotic\_value} \tag{13}$$

Through iteration, g is reduced from 2.5 to 0 in a way that is not linear, i.e., in both the exploitation and exploration phases. Randomized vectors in the interval [0,1] are b_1 and b_2. Finally, the effect of sexual drive on chimpanzees' ability to hunt is represented by the chaotic vector c, computed using the various chaotic maps.

In the standard population-based optimization technique, particles (i.e., chimpanzees) behave similarly for local and global searches. This allows for a single search strategy to be used for both. Different groups working independently toward a shared objective can be employed in any population-based optimization technique to get both a deterministic and stochastic search outcome. Different chimpanzee communities employ a unique set of tactics to update g. When updating the autonomous groups, any continuous function will get executed. These operations must be chosen so that g decreases with each repetition.

As a whole, these four subsets use their unique methodologies to explore distinct areas of the search area. Additionally, the best variants of RCO with various autonomous groups are selected from among the many techniques that have been assessed. Table 1 and Figure 3 displayed the dynamical coefficients of g. The current iteration is displayed as f, while the maximal number of iterations is indicated by F. Each group of autonomous explorers has its unique behavior thanks to the dynamic coefficients selected with varying curves and slopes to maximize the effectiveness of RCOs.

Eqn. (9) and Eqn. (10) depict the chimpanzees in two dimensions and a three-dimensional display, along with various probable future places for the animal. By modifying the parameters of the d and u vectors, a chimpanzee in the location (p, q) can move about the $(p*, q*)$ location of its prey. It is important to keep in mind that the randomized vectors b_1 and b_2 provide the chimps access to any location in the search space. The scope of this idea may be extended to t -dimensional search spaces.

3.2.2. Exploration

First, the chimps will investigate the prey's position (by driving, blocking, and chasing), and second, they could encircle it, both of which are modeled mathematically. $Atkr$'s are the ones who often oversee the search. Sometimes, the $Drvr$, the $Barr$, and the $Chsr$ join the hunting process. Initial iterations provide no clues regarding the position of prey to achieve maximum success. The victim (i.e., prey) is believed to be in a defensive position to address this deficiency. The $Atkr$'s location should then be used to revise the positions of the $Drvr$, the $Barr$, and the $Chsr$. Therefore, the top four answers are saved, and the other chimpanzees are compelled to adjust their positions to match those of the top performers. Eqn.(14) to Eqn.(22) outline the parameters of RCO:

$$y_{Atkr} = |U_1 P_{Atkr} - c_1 y| \tag{14}$$

$$y_{Barr} = |U_2 P_{Barr} - c_2 P| \tag{15}$$

$$y_{Chsr} = |U_3 P_{Chsr} - c_2 P| \tag{16}$$

$$y_{Drvr} = |U_4 P_{Drvr} - c_4 P| \quad (17)$$

$$P_1 = P_{Atkr} - d_1(y_{Atkr}) \quad (18)$$

$$P_2 = P_{Barr} - d_2(y_{Barr}) \quad (19)$$

$$P_3 = P_{Chsr} - d_3(y_{Chsr}) \quad (20)$$

$$P_4 = P_{Drvr} - d_4(y_{Drvr}) \quad (21)$$

$$P(f+1) = \frac{P_1 + P_2 + P_3 + P_4}{4} \quad (22)$$

Search agents (chimp) position in the search area is updated based on the locations of other chimps. The $Atkr$, the $Barr$, the $Chsr$, and the $Drvr$'s all move in a circle, and the chimp's ultimate location is completely random.

3.2.3. Exploitation

As previously said, once the victim stops moving, the chimpanzees will pounce on it and end the hunt. The attacking process may be modeled numerically by decreasing the value of g in a linear fashion. Remember that the d vector has the same limited range as the g vector. More specifically, d is a variable in the range $[-2g\ ,\ 2g]$, whereas g decreases from 2.5 to 0 over time. If the random numbers of d fall between the interval $[1, 1]$.

The future location of a chimpanzee ranges from its present location to the prey's location. The possibility of being stuck in local minima exists in RCO, even though the suggested $Drvr$, $Barr$, and $Chsr$ techniques do uniquely improve exploration capabilities. Thus, a different operator is needed to highlight the exploratory capabilities "in the exploitation phase." This means that RCO, in addition to the operators in the exploration phase, requires a second operator in the exploitation phase that can avoid local minimum entrapment.

The chimpanzees in RCO split apart to search the prey and attack the same as a group. To mathematically represent this behavior, the vectors of d are allotted in such a way that the contradiction$|d| > 1$ causes chimps to disperse from prey (i.e., local optima avoidance), and the inequality $|d| < 1$ force chimps to concentrate on prey position (i.e., global optima).

The exploring phase of RCO aids the u vector. In the range [0, 2], the random vector u is represented by using Eqn. (10). This vector gives prey irrational weights that either increase $(u > 1)$ or decrease $(u < 1)$. The importance of the prey's position in the distance specification given by Eqn. (14) to Eqn. (17). In the wild, chimpanzees are prevented from reaching their prey by a vector of u. This means that the random weight applied by the vectors of u to the prey can either make or avoid the hunt.

3.2.4. Social Incentive-based Exploitation

The chimpanzee community relies on meat hunting as a social incentive (sex, grooming, etc.). Chimpanzees would leave their hunts to try to steal the meat from the last stage. As a result, in a state of utter chaos, they attempt to get hunting meat for gastronomic purposes. Last-stage chimpanzee behavior like this may be mimicked with chaotic maps.

The deterministic processes present in RCO give rise to the unanticipated behavior of hunting the prey. The chaotic maps present in RCO is designed for beginning with an initial value of 0.8. Within this approach, the update procedure of RCO is expressed as Eqn. (23).

$$P_{chimp}(f+1) = \begin{cases} P_{prey}(f) - d.y & if\ \ \vartheta < 0.4 \\ Chaotic_{Value} & if\ \vartheta > 0.4 \end{cases} \quad (23)$$

wherein ϑ is an arbitrary number between zero and one.

3.2.5. Fusion of RCO for FFNN

Each chimpanzee in $RCO - FFNN$ represents a potential neuron in $FFNN$, complete with connection weights and biases, recorded as a one-dimensional vector. In the $FFNN$, the height of each vector is specified by the sum of its weights and biases, which is equal to the distance, which is expressed in Eqn. (24).

$$Distance = (t \times l) + (2 \times l) + 1 \quad (24)$$

where t is the count of inputs and l is the number of neurons located in the hidden layer. Eqn. (25) provides the $RCO - FFNN$'s final vector.

$$chimp = [N_1 N_2 N_3 \ldots\ldots N_{11} N_{12} v_1 v_2 v_3 v_4 v_5 v_6] \quad (25)$$

$RCO - FFNN$'s search agents assess each training sample against a predefined fitness function. The Mean Square Error (MSE) fully quantifies the discrepancy between the intended and evaluated values. The mean squared error is mathematically expressed as Eqn. (26).

$$MSE = \frac{1}{c}\sum_{s=1}^{c}(g - \hat{g})^2 \quad (26)$$

where the target value is indicated as g, and the evaluation value is indicated as $\hat{g}$, and the sample size is c.

4. About the Dataset

Data aggregation from many MRI scanners was a valuable and successful endeavor in ABIDE I. However, the complexity of the connectome, the wide heterogeneity of ASD, and the first results of the ABIDE I data analysis all indicate the need for much larger and better-characterized samples.

Thus, ABIDE II was established at the National Institute of Mental Health (R21MH107045) to continue exploratory study on the ASD brain connectome. Since its inception, ABIDE II has included over a thousand datasets with phenotypic characterization, particularly those evaluating core ASD and concomitant symptoms. Moreover, the data consists of two sets, each of which is a longitudinal sample of 38 people spread across a time (1 to 4-year interval). There are currently 19 locations participating in ABIDE II (10 charter institutions and 7 new members), and these sites have provided 1114 datasets, including data on 521 persons with ASD and 593 controls (age range: 5-64 years). Researchers have had access to this data since June 2016. Following HIPAA and the guidelines employed by the 1000 Functional Connectomes Project/INDI, none of the datasets contains any personally identifying information. Figure 2 provides the sample images. The fMRI images hold pixel values of 256×256.

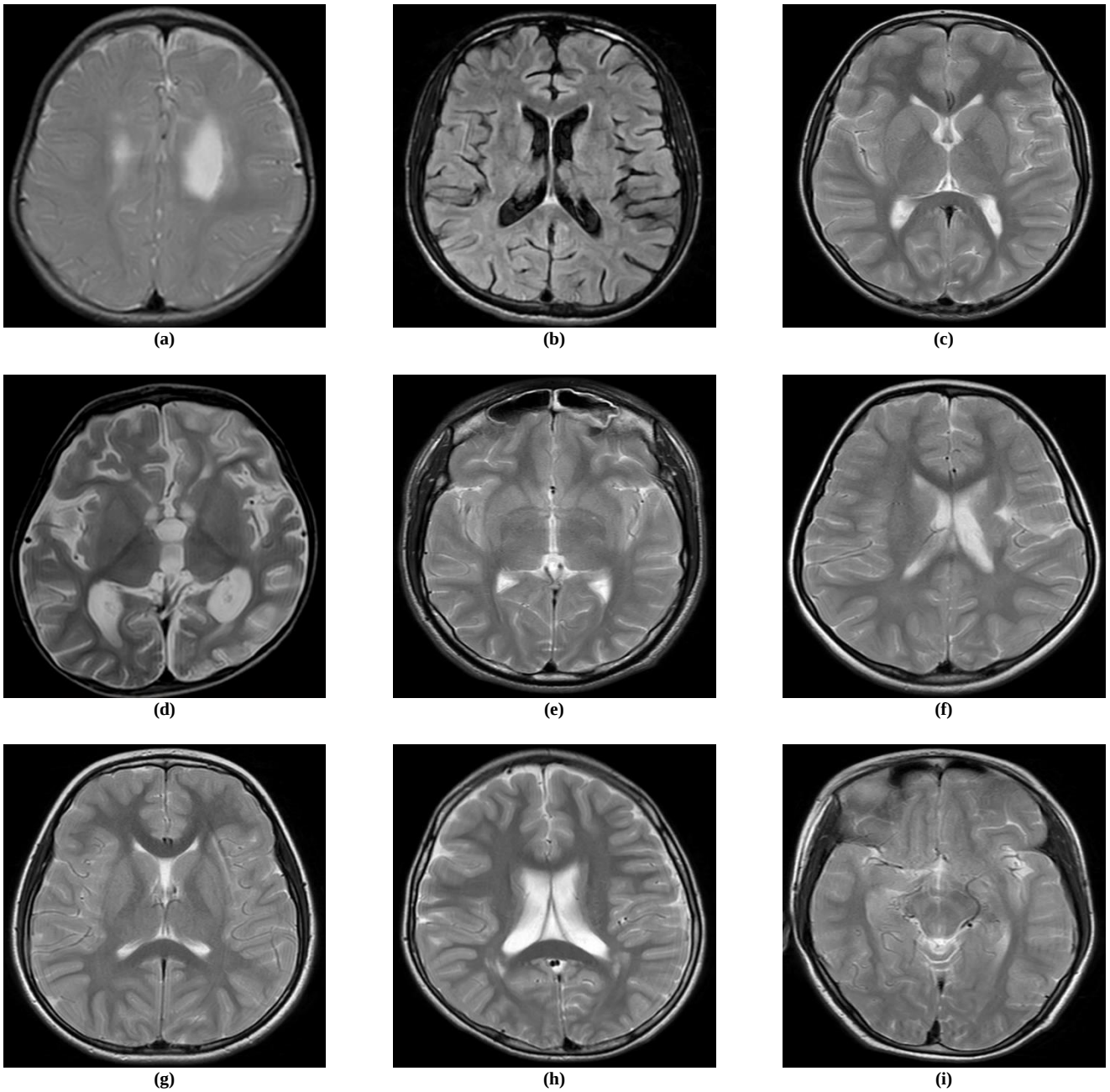

(a) **(b)** **(c)** **(d)** **(e)** **(f)** **(g)** **(h)** **(i)**

Fig. 2 Autistic fMRI Brain Images

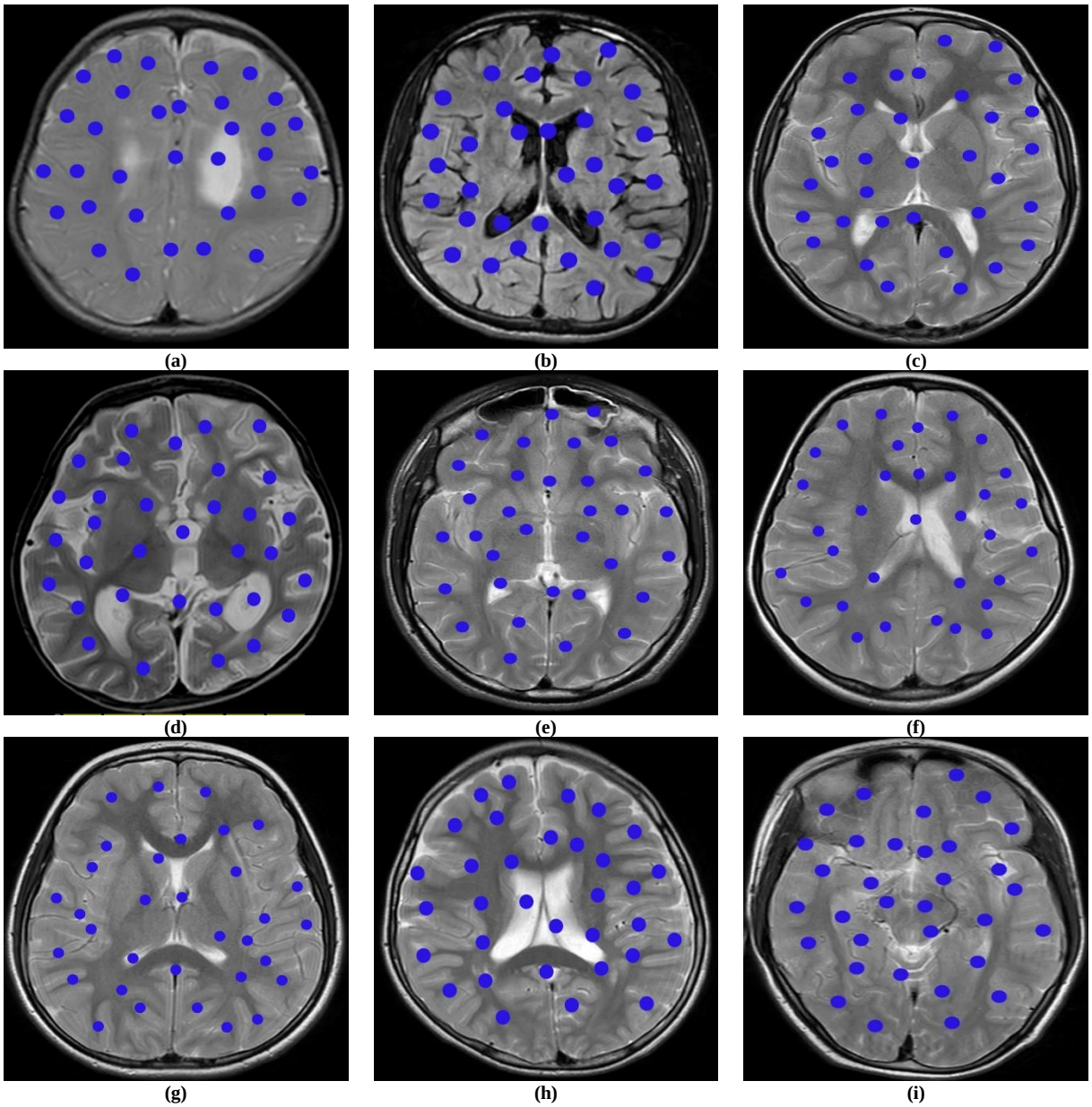

Fig. 3 Autistic Brain Regions detected by $RCO - FFNN$

5. Performance Metrics

To compare how well ZBSO-RMLPNN performs than GERSVM and FC-CNM, the current study uses the standard sum benchmark performance criteria listed below.

- Classification Accuracy ($Cl - Acc$): The effectiveness of a classification model may be measured by looking at the proportion of right predictions among all predictions.
- F-Measure ($F - Msr$): It combines a classifier's recall and precision results into a single statistic by calculating their harmonic mean.
- Fowlkes-Mallows Index (FMI): It indicates the recall and precision results geometric mean.
- Matthews Correlation Coefficient (MCC): It indicates the quality measure in classification with binary class.

True-positive ($Tr - Pos$), False-positive ($Fl - Pos$), True-Negative ($Tr - Neg$), and False-Negative ($Fl - Neg$) are the four variables applied in the calculation of aforementioned performance metrics.

6. Results and Discussion

6.1. ASD detection by ZPSO-RMLPNN

Figure 3 highlights the autistic brain regions that are identified by the proposed classifier RCO-FFNN while evaluating in MATLAB 2021b.

Table 1. $Tr-Pos$and $Fl-Pos$ Result Values

Classifiers	$Tr-Pos$	$Fl-Pos$
GERSVM	33.752	17.953
FC-CNM	36.266	15.081
RCO-FFNN	42.998	8.618

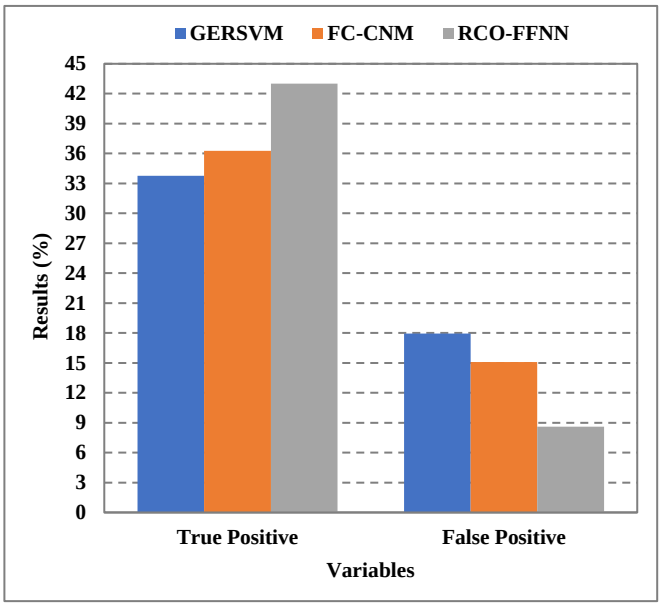

Fig. 4 $Tr-Pos$and $Fl-Pos$ analysis

Table 2. $Tr-Neg$and $Fl-Neg$ Result Values

Classifiers	$Tr-Neg$	$Fl-Neg$
GERSVM	30.969	17.325
FC-CNM	34.470	14.183
RCO-FFNN	40.395	7.989

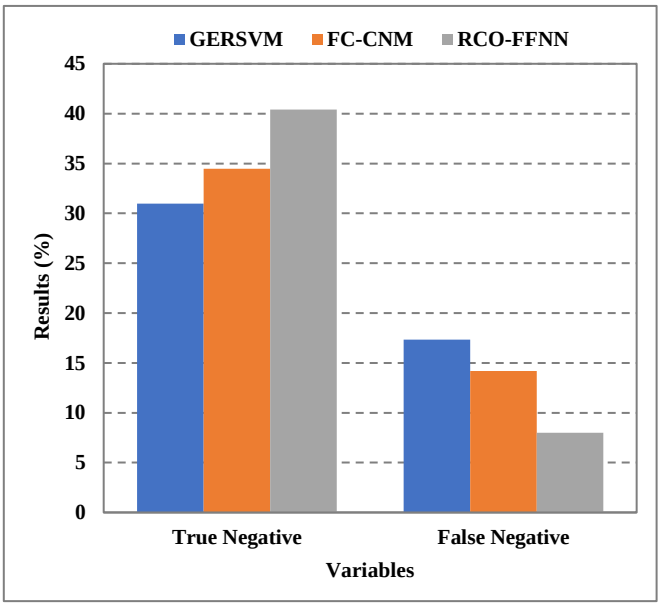

Fig. 5 Tr – Negand Fl – Neg analysis

6.2. Positivity Analysis

Figure 4 examines the classifier assessment positive results (i.e., $Tr-Pos$ and $Fl-Pos$). $Tr-Pos$ and $Fl-Pos$ are the variables that are plotted along the $X-axis$. The $Y-axis$ displays the percentage of results obtained in $Tr-Pos$ and $Fl-Pos$.

From Figure 4, it is easy to deduce that the proposed classifier provides superior Tr-Pos and Fl-Pos performance to both $GERSVM$ and $FC-CNM$. $RCO-FFNN$ outperforms $GERSVM$ and $FC-CNM$ in detecting ASD and $non-ASD$ because of its optimization-based categorization. GERSVM and FC-CNM do not apply any optimization algorithms, leading to unsatisfactory $Tr-Pos$ and $Fl-Pos$ in ASD and $non-ASD$ detection. Table 1 illustrates the obtained result values of $Tr-Pos$ and $Fl-Pos$ during the evaluation.

6.3. Negativity Analysis

Figure 5 analyzes the negative results (i.e., $Tr-Neg$and $Fl-Neg$) obtained during the evaluation of classifiers. The $X-axis$ is plotted with $Tr-Neg$and $Fl-Neg$, which are variables. $Y-axis$ is plotted with results measured in percentage.

Figure 5 shows that the proposed classifier does better classification than $GERSVM$ and $FC-CNM$ in terms of $Tr-Neg$and $Fl-Neg$.

The convergence function present in RCO-FFNN assists in identifying which fMRI does not meet ASD and non-ASD (i.e., $Tr-Neg$and $Fl-Neg$). $GERSVM$ and $FC-CNM$ do not apply any special function to differentiate ASD and $non-ASD$. The values of $Tr-Neg$and $Fl-Neg$results that were determined during the evaluation of classifiers are included in Table 2.

6.4. Cl – Acc and F – Msr Analysis

Figure 6 compares the $Cl-Acc$ and $F-Msr$ findings of the proposed classifier to those of the existing classifiers. The $x-axis$ is labeled with $Cl-Acc$ and $F-Msr$, while the y-axis shows the proportion of attained outcomes. Figure 6 makes it abundantly evident that the suggested classifier performs better in terms of the $Cl-Acc$ and $F-Msr$ than $GERSVM$ and $FC-CNM$. The exploration and exploitation phase assists RCO-FFNN in giving maximum$Cl-Acc$ and $F-Msr$. $RCO-FFNN$ considers ASD as prey and attempts to classify it more accurately. $GERSVM$ and $FC-CNM$ do not explore and exploit the dataset to fix ASD and non-ASD, which results in poor $Cl-Acc$ and $F-Msr$. The attained $Cl-Acc$ and $F-Msr$ values during classifier assessment are listed in Table 3.

Table 3. Cl – Acc and F – Msr Result Values

Classifiers	$Cl-Acc$	$F-Msr$
GERSVM	64.722	65.677
FC-CNM	70.736	71.252
RCO-FFNN	83.393	83.815

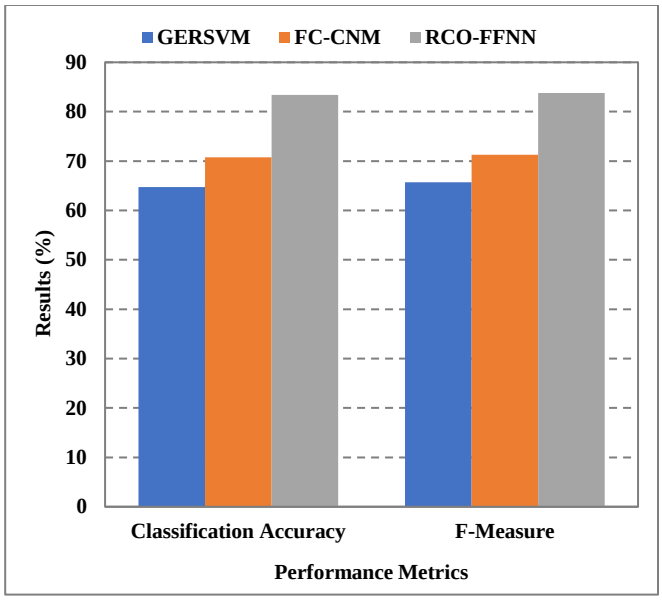

Fig 6 Cl − Acc and F − Msr analysis

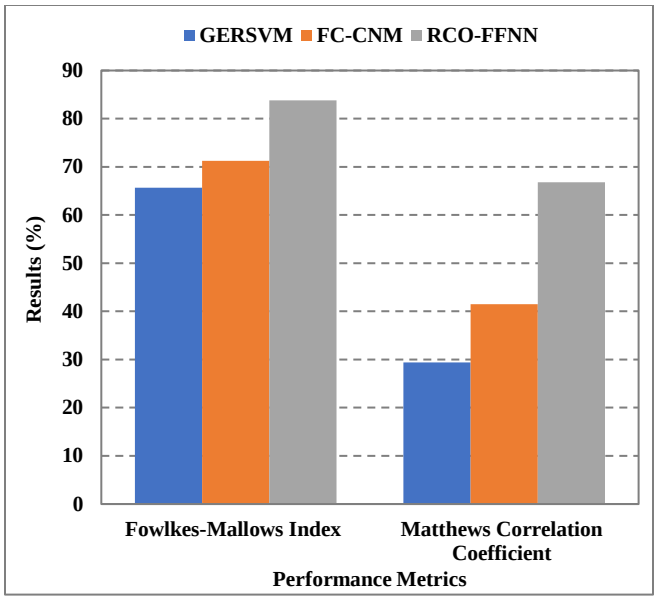

Fig. 7 FMI and MCC analysis

6.5. FMI and MCC Analysis

A comparison of proposed and current classifiers for FMI and MCC outcomes is shown in Figure 7. FMI and MCC metrics are shown on the $X - axis$, while the outcomes are shown on the $Y - axis$.

As shown in Figure 7, the suggested classifier achieves higher FMI and MCC results than both $GERSVM$ and $FC - CNM$. Exploitation motivated by social incentives in $RCO - FFNN$ plays a significant role in achieving better FMI and MCC. $GERSVM$ and $FC - CNM$ do not perform classification in an optimistic manner which leads to poor FMI and MCC. Table 4 displays the results obtained for both proposed and existing classifiers for the FMI and MCC metrics.

Table 4. FMI and MCC Result Values

Classifiers	FMI	MCC
GERSVM	65.678	29.394
FC-CNM	71.255	41.465
RCO-FFNN	83.816	66.770

7. Conclusion

ASD refers to a spectrum of conditions that affect brain development. It manifests in infancy and progresses throughout one's life; early diagnosis is key to effective therapy and a speedy recovery. Using medical image mining strategies, these deficiencies may be identified. This paper proposes RCO-FFNN to identify ASD and non-ASD more accurately with ABIDE II dataset. RCO-FFNN is a fusion of Feed Forward Neural Network and enriched chimp optimization, namely, rapturous chimp optimization. fMRI images are deeply analyzed and classified using exploration and exploitation phases in the proposed optimization-based classifier RCO-FFNN.

While evaluating the RCO-FFNN against the current classifiers with the ABIDE-II dataset, it is identified that the RCO-FFNN has achieved 83.393% classification accuracy, 83.815% of F-Measure, 83.816% of Fowlkes-Mallows Index, and 66.77% of Matthews Correlation Coefficient. The future scope of this research work can be focused on different bio-inspired strategies fusing with the convolutional neural network.

References

[1] Mariam M. Hassan, and Hoda M. O. Mokhtar, "Investigating Autism Etiology and Heterogeneity by Decision tree Algorithm," *Informatics in Medicine Unlocked*, vol. 16, p. 100215, 2019. [CrossRef] [Google Scholar] [Publisher link]

[2] Jiannan Kang et al., "The Study of the Differences Between Low-functioning Autistic Children and Typically Developing Children in the Processing of the Own-race and Other-race faces by the Machine Learning Approach," *Journal of Clinical Neuroscience*, vol. 81, pp. 54–60, 2020. [CrossRef] [Google Scholar] [Publisher link]

[3] Elyza Kelly, Christine Ochoa Escamilla, and Peter T. Tsai, "Cerebellar Dysfunction in Autism Spectrum Disorders: Deriving Mechanistic Insights from an Internal Model Framework," *Neuroscience*, vol. 462, pp. 274–287, 2021. [CrossRef] [Google Scholar] [Publisher link]

[4] E. Puerto et al., "Using Multilayer Fuzzy Cognitive Maps to diagnose Autism Spectrum Disorder," *Applied Soft Computing*, vol. 75, pp. 58–71, 2019. [CrossRef] [Google Scholar] [Publisher link]

[5] Roberto Munoz et al., "Developing Computational Thinking Skills in Adolescents with Autism Spectrum Disorder Through Digital Game Programming," *IEEE Access*, vol. 6, pp. 63880–63889, 2018. [CrossRef] [Google Scholar] [Publisher link]

[6] Amani Induni Soysa, and Abdullah Al Mahmud, "Technology for Children with Autism Spectrum Disorder: What Do Sri Lankan Parents and Practitioners Want?," *Interacting with Computers*, vol. 31, no. 3, pp. 282–302, 2019. [CrossRef] [Google Scholar] [Publisher link]

[7] Sonia Cerullo et al., "Acting with Shared Intentions: A Systematic Review on Joint Action Coordination in Autism Spectrum Disorder," *Brain Cognition*, vol. 149, p. 105693, 2021. [CrossRef] [Google Scholar] [Publisher link]

[8] Michal T. Tomczak et al., "Stress Monitoring System for Individuals with Autism Spectrum Disorders," *IEEE Access*, vol. 8, pp. 228236–228244, 2020. [CrossRef] [Google Scholar] [Publisher link]

[9] Sarah E. Frampton et al., "Autism Spectrum Disorder," *Reference Module in Neuroscience and Biobehavioral Psychology*, 2022. [CrossRef] [Publisher link]

[10] Nazreem Rusli et al., "Implementation of Wavelet Analysis on Thermal Images for Affective States Recognition of Children with Autism Spectrum Disorder," *IEEE Access*, vol. 8, pp. 120818–120834, 2020. [CrossRef] [Google Scholar] [Publisher link]

[11] Shuaibing Liang et al., "Autism Spectrum Self-Stimulatory Behaviors Classification Using Explainable Temporal Coherency Deep Features and SVM Classifier," *IEEE Access*, vol. 9, pp. 34264–34275, 2021. [CrossRef] [Google Scholar] [Publisher link]

[12] Luis Roberto Ramos-Aguiar, and Francisco Javier Alvarez-Rodrguez, "Teaching Emotions in Children with Autism Spectrum Disorder Through a Computer Program with Tangible Interfaces," *IEEE Revista Iberoamericana de Tecnolgias del Aprendizaje*, vol. 16, no. 4, pp. 365–371, 2021. [CrossRef] [Google Scholar] [Publisher link]

[13] Andre Klapper et al., "The Control of Automatic Imitation Based on Bottom-up and Top-down Cues to Animacy: Insights from Brain and Behavior," *Journal of Cognitive Neuroscience*, vol. 26, no. 11, pp. 2503–2513, 2014. [CrossRef] [Google Scholar] [Publisher link]

[14] Qiao Ke et al., "Adaptive Independent Subspace Analysis of Brain Magnetic Resonance Imaging Data," *IEEE Access*, vol. 7, pp. 12252–12261, 2019. [CrossRef] [Google Scholar] [Publisher link]

[15] R. Surendiran et al., "Effective Autism Spectrum Disorder Prediction to Improve the Clinical Traits using Machine Learning Techniques," *International Journal of Engineering Trends and Technology*, vol. 70, no. 4, pp. 343-359, 2022. [CrossRef] [Google Scholar] [Publisher link]

[16] Qiang Wang, and Olga Sourina, "Real-Time Mental Arithmetic Task Recognition from EEG Signals," *IEEE Transactions on Neural Systems and Rehabilitation Engineering*, vol. 21, no. 2, pp. 225–232, 2013. [CrossRef] [Google Scholar] [Publisher link]

[17] Haik Kalantarian et al., "A Mobile Game for Automatic Emotion-Labeling of Images," *IEEE Transactions on Games*, vol. 12, no. 2, pp. 213–218, 2020. [CrossRef] [Google Scholar] [Publisher link]

[18] Yize Zhao, Jian Kang, and Qi Long, "Bayesian Multiresolution Variable Selection for Ultra-High Dimensional Neuroimaging Data," *IEEE/ACM Transaction on Computational Biology Bioinformatics*, vol. 15, no. 2, pp. 537–550, 2018. [CrossRef] [Google Scholar] [Publisher link]

[19] Bogdan Alexandru Cociu et al., "Multimodal Functional and Structural Brain Connectivity Analysis in Autism: A Preliminary Integrated Approach with EEG, fMRI, and DTI," *IEEE Transactions on Cognitive and Developmental Systems*, vol. 10, no. 2, pp. 213–226, 2018. [CrossRef] [Google Scholar] [Publisher link]

[20] Pradeep Raj Krishnappa Babu, and Uttama Lahiri, "Multiplayer Interaction Platform with Gaze Tracking for Individuals with Autism," *IEEE Transactions on Neural Systems and Rehabilitation Engineering*, vol. 28, no. 11, pp. 2443–2450, 2020. [CrossRef] [Google Scholar] [Publisher link]

[21] Faisal Mehmood et al., "Dominance in Visual Space of ASD Children Using Multi-Robot Joint Attention Integrated Distributed Imitation System," *IEEE Access*, vol. 7, pp. 168815–168827, 2019. [CrossRef] [Google Scholar] [Publisher link]

[22] Sara Ali et al., "A Preliminary Study on Effectiveness of a Standardized Multi-Robot Therapy for Improvement in Collaborative Multi-Human Interaction of Children with ASD," *IEEE Access*, vol. 8, pp. 109466–109474, 2020. [CrossRef] [Google Scholar] [Publisher link]

[23] M. Oliveira, M. Guebert, and P. Nohama, "TEACCH Methodology-Based Web System to Support Learning for Children with Autism," *IEEE Latin America Transactions*, vol. 16, no. 11, pp. 2698–2705, 2018. [CrossRef] [Google Scholar] [Publisher link]

[24] Md Rishad Ahmed et al., "Single Volume Image Generator and Deep Learning-Based ASD Classification," *IEEE Journal of Biomedical and Health Informatics*, vol. 24, no. 11, pp. 3044–3054, 2020. [CrossRef] [Google Scholar] [Publisher link]

[25] Olivier Le Meur et al., "From KannerAustim to Asperger Syndromes, the Difficult Task to Predict Where ASD People Look at," *IEEE Access*, vol. 8, pp. 162132–162140, 2020. [CrossRef] [Google Scholar] [Publisher link]

[26] Jun Wang et al., "Multi-Class ASD Classification Based on Functional Connectivity and Functional Correlation Tensor via Multi-Source Domain Adaptation and Multi-View Sparse Representation," *IEEE Transactions on Medical Imaging*, vol. 39, no. 10, pp. 3137–3147, 2020. [CrossRef] [Google Scholar] [Publisher link]

[27] Katrin Solveig Lohan et al., "Toward Improved Child–Robot Interaction by Understanding Eye Movements," *IEEE Transactions on Cognitive and Developmental Systems*, vol. 10, no. 4, pp. 983–992, 2018. [CrossRef] [Google Scholar] [Publisher link]

[28] J. Ramkumar, and R. Vadivel, "Bee Inspired Secured Protocol for Routing in Cognitive Radio ad Hoc Networks," *Indian Journal of Science and Technology*, vol. 13, no. 30, pp. 3059-3069, 2020. [CrossRef] [Google Scholar] [Publisher link]

[29] J. Ramkumar, and R. Vadivel, "Improved frog Leap Inspired Protocol (IFLIP) – for Routing in Cognitive Radio ad Hoc Networks (CRAHN)," *World Journal of Engineering*, vol. 15, no. 2, pp. 306–311, 2018. [CrossRef] [Google Scholar] [Publisher link]

[30] J. Ramkumar, and R. Vadivel, "Multi-Adaptive Routing Protocol for Internet of Things based Ad-hoc Networks," *Wireless Personal Communications*, vol. 120, pp. 887–909, Apr. 2021. [CrossRef] [Google Scholar] [Publisher link]

[31] Ramkumar Jaganathan, and Ramasamy Vadivel, "Intelligent Fish Swarm Inspired Protocol (IFSIP) for Dynamic Ideal Routing in Cognitive Radio Ad-Hoc Networks," *International Journal of Computing Digital Systems*, vol. 10, no. 1, pp. 1063–1074, 2021. [CrossRef] [Google Scholar] [Publisher link]

[32] Ramkumar Jaganathan, and Vadivel Ramasamy, "Performance Modeling of Bio-inspired Routing Protocols in Cognitive Radio Ad Hoc Network to Reduce End-to-end Delay," *International Journal of Intelligent Engineering and Systems*, vol. 12, no. 1, pp. 221–231, 2019. [CrossRef] [Google Scholar] [Publisher link]

[33] J. Ramkumar, and R. Vadivel, "CSIP—cuckoo Search Inspired Protocol for Routing in Cognitive Radio ad Hoc Networks," *Advances in Intelligent Systems and Computing*, vol. 556, 2017. [CrossRef] [Google Scholar] [Publisher link]

[34] J. Ramkumar et al., "Energy Consumption Minimization in Cognitive Radio Mobile Ad-Hoc Networks using Enriched Ad-hoc On-demand Distance Vector Protocol," *2022 International Conference on Advanced Computing Technologies and Applications (ICACTA)*, 2022. [CrossRef] [Google Scholar] [Publisher link]

[35] J. Ramkumar, and R. Vadivel, "Whale Optimization Routing Protocol for Minimizing Energy Consumption in Cognitive Radio Wireless Sensor Network," *International Journal of Computer Networks and Applications*, vol. 8, no. 4, pp. 455–464, 2021. [CrossRef] [Google Scholar] [Publisher link]

[36] J. Ramkumar, and R. Vadivel, "Meticulous Elephant Herding Optimization based Protocol for Detecting Intrusions in Cognitive Radio Ad Hoc Networks," *International Journal of Emerging Trends in Engineering Research*, vol. 8, no. 8, pp. 4548–4554, 2020. [CrossRef] [Google Scholar] [Publisher link]

[37] J. Ramkumar et al., "IoT-Based Kalman Filtering and Particle Swarm Optimization for Detecting Skin Lesion," *Lecture Notes in Electrical Engineering*, vol. 975, 2023. [CrossRef] [Google Scholar] [Publisher link]

[38] Xia-an Bi et al., "The Genetic-Evolutionary Random Support Vector Machine Cluster Analysis in Autism Spectrum Disorder," *IEEE Access*, vol. 7, pp. 30527–30535, 2019. [CrossRef] [Google Scholar] [Publisher link]

[39] N. Chaitra, P. A. Vijaya, and Gopikrishna Deshpande, "Diagnostic Prediction of Autism Spectrum Disorder using Complex Network Measures in a Machine Learning Framework," *Biomedical Signal Processing and Control*, vol. 62, p. 102099, 2020. [CrossRef] [Google Scholar] [Publisher link]

[40] Masakazu Hirokawa et al., "Adaptive Behavior Acquisition of a Robot Based on Affective Feedback and Improvised Teleoperation," *IEEE Transactions on Cognitive and Developmental Systems*, vol. 11, no. 3, pp. 405–413, 2019. [CrossRef] [Google Scholar] [Publisher link]